Atomic Data and Nuclear Data Tables 120 (2018) 121–151

Contents lists available at ScienceDirect

Atomic Data and Nuclear Data Tables

journal homepage: www.elsevier.com/locate/adt

Differential and total cross sections and astrophysical *S*-factors for $^{2}H(d,n)^{3}He$ and $^{2}H(d,p)^{3}H$ reactions in a wide energy range

P.R. Goncharov

Research Laboratory for Controlled Nuclear Fusion, Peter the Great Saint Petersburg Polytechnic University, 29 Polytechnicheskaya st., Saint Petersburg 195251, Russian Federation

ARTICLE INFO

Article history:
Received 6 April 2017
Received in revised form 16 May 2017
Accepted 16 May 2017
Available online 17 June 2017

Keywords:
Nuclear fusion
Deuteron–deuteron reactions
c.m. differential cross sections
Primordial nucleosynthesis

ABSTRACT

Differential cross sections of deuteron–deuteron fusion reactions are needed in astrophysics, precision cosmology, nuclear physics, and controlled nuclear fusion research. New parametrizations for center of mass differential cross sections, total cross sections and astrophysical *S*-factors in a wide range of specific energy from 0.5 keV/u to about 0.5 GeV/u have been obtained. Straightforward approximating formulae readily suitable for multithreaded algorithmization are given here for $^{2}H(d,n)^{3}He$ and $^{2}H(d,p)^{3}H$ reactions. The energy range is about two orders of magnitude broader than that in the tables published earlier for neutron branch.

E-mail address: p.goncharov@spbstu.ru.

http://dx.doi.org/10.1016/j.adt.2017.05.006
0092-640X/

Contents

1. Introduction

Deuteron–deuteron reactions ^{2}H(d,n)^{3}He and ^{2}H(d,p)^{3}H are among the nuclear processes responsible for the production of light elements in Standard Big Bang Nucleosynthesis [1,2]. Thus, rates of these reactions are important in nuclear astrophysics and precision cosmology for a quantitative description of the early Universe [3]. Another subject is the deuterium burning in the pre-main-sequence phase of stellar evolution [4]. Earlier works such as [5,6] and newer studies [7,8] consider cross sections and reaction rates in the energy region relevant for astrophysics. Extended parametric fits to the astrophysical S-factors and, therefore, the total cross sections were published in Ref. [9] for a much wider range of energies.

The reactions considered here are also of interest from the viewpoint of nuclear structure and fundamental symmetry principles, as indicated in work [10]. The symmetry of the angular distribution of the products of these reactions about 90° in the center of mass frame is one of characteristic properties [10,11]. Regarding the question of charge symmetry, its violations are known to be due to the perturbing effects of the mass difference between up and down quarks and electromagnetic interactions between the quarks [12]. Charge symmetry violation in reactions ^{2}H(d,n)^{3}He and ^{2}H(d,p)^{3}H was addressed in [13,14] and more recently in Ref. [15].

Calculations of nuclear fusion reaction rates, together with energetic and angular distributions of the products of these reactions, are an essential part of the physics basis for the ongoing work on neutron sources, demonstration power plant concepts and

fusion–fission hybrid systems based on magnetic plasma confinement [16,17], for the development of blankets of such systems [18–20], and for the advancement of nuclear technologies of the controlled fusion [21–23]. These calculations are also necessary for the analysis of data of neutron spectrometry of fusion plasma [24,25]. Along with the energy spectra of neutrons, which are among the key characteristics of the reactor, distributions of charged fusion products are also addressed in the literature, because not only they contribute to the fast ion population in the plasma, if they are confined, but they also significantly influence the first wall, if they are not confined. Therefore, calculations of spatial, energetic and angular distributions of the sources of nuclear fusion products are necessary for experimental and theoretical investigations of the confinement of fast particles, associated heating and the ignition condition [26–28].

In addition, besides fundamental research and technological applications, neutrons produced in fusion reactions may be used for medical purposes [29–31]. In this respect the knowledge of differential cross sections is also needed to calculate the source spectrum influencing the therapeutic effect.

Experimental data on differential cross sections of the mentioned reactions, theoretical analysis and approximating formulae are present in a wide variety of bibliographic sources, including periodicals, reports and compilations. In a systemized form, the data was presented earlier in the well-known work [32]. Afterwards, as the tables of differential cross sections were amended, updated parametrizations were published in the IAEA report [33], and later in Ref. [34]. The most recent IAEA update on the absolute angle-dependent differential cross sections so far is Ref. [35]. These compilations concern neutron source reactions including ^{2}H(d,n)^{3}He. The data for the proton branch ^{2}H(d,p)^{3}H is nearly as abundant in the bibliography, however, there are no systemized tables or formulae covering a wide energy range for this case.

The purpose of this article is to present the straightforward approximating formulae suitable for parallel algorithmization for differential cross sections of the two main branches of the deuterium–deuterium fusion reaction. The energy range is almost two orders of magnitude broader than that in Ref. [35], where the recommended energy dependences were given in the form of tables rather than formulae. A number of additional bibliographic sources have been included in the data set. Parametrizations for total cross sections and astrophysical S-factors are also given for the energy range extended by about two orders of magnitude in comparison with work [36].

2. Overview of bibliographic sources

Theoretical treatments of differential cross sections of the deuterium–deuterium reactions were given in renowned publications [37–40]. The most recent developments of theoretical calculations are described in works [41–43] and references therein. These calculations are using the approach of Ref. [44] based on work [45]. Asymptotic behavior of the differential cross sections is discussed in Ref. [46] in terms of the quark–gluon picture of nuclei.

Experimental data on the differential cross sections as functions of the specific energy $\mathscr{E}$ and the polar angle ϑ in the center of mass frame are typically fitted with an expansion in a truncated series of Legendre polynomials

$$\frac{d\sigma(\mathscr{E},\vartheta)}{d\Omega_{\mathrm{c.m.}}} = \sum_{j=0}^{L} A_{2j}(\mathscr{E}) P_{2j}(\cos\vartheta), \tag{1}$$

reminiscent of what is used in partial wave decomposition, with only even terms owing to the equivalence of ϑ and $(\pi-\vartheta)$, i.e. the symmetry about 90°, associated with the identity of target and projectile deuterons.

Unpolarized cross sections averaged over the spins of deuterons are implied herewith. Nuclear fusion utilizing spin-polarized fuel particles, thoroughly discussed in review [47] and in monograph [48], is beyond the scope of this article. Azimuthal symmetry is assumed in Eq. (1).

In Refs. [32–35] dimensionless normalized Legendre coefficients $a_{2j}(\mathscr{E}) = A_{2j}(\mathscr{E})/\sum_{l=0}^{L} A_{2l}(\mathscr{E})$ are used. Since all Legendre polynomials equal unity at 0°, the normalizing denominator equals the differential cross section at 0°, i.e. $\frac{d\sigma(\mathscr{E},0^\circ)}{d\Omega_{\mathrm{c.m.}}} = \sum_{l=0}^{L} A_{2l}(\mathscr{E})$. Obviously,

$$\sum_{j=0}^{L} a_{2j}(\mathscr{E}) = 1 \tag{2}$$

by definition. The differential cross section is then

$$\frac{d\sigma(\mathscr{E},\vartheta)}{d\Omega_{\mathrm{c.m.}}} = \frac{d\sigma(\mathscr{E},0^\circ)}{d\Omega_{\mathrm{c.m.}}} \sum_{j=0}^{L} a_{2j}(\mathscr{E}) P_{2j}(\cos\vartheta). \tag{3}$$

Bearing in mind the orthogonality of Legendre polynomials and the trivial integration over the azimuthal angle due to symmetry, for the total cross section we have

$$\sigma(\mathscr{E}) = 4\pi a_0(\mathscr{E}) \frac{d\sigma(\mathscr{E},0^\circ)}{d\Omega_{\mathrm{c.m.}}}. \tag{4}$$

For reaction ^{2}H(d,n)^{3}He recommended Legendre coefficients given in work [32] are defined from 10 keV/u to 5 MeV/u. Within this range the coefficients from report [33] basically follow ones from Ref. [32], while for higher values of the specific energy up to 7.5 MeV/u they follow the work [49]. Coefficients from report [34] are defined in a wider range of specific energies up to 20 MeV/u. Below 7.5 MeV/u they agree with publication [33]. In the higher energy region from 10 MeV/u to 20 MeV/u they follow the work [50], based on earlier data from Ref. [51]. In publication [35] tables of the coefficients were amended and the energy range was somewhat further extended from about 1 keV/u up to 50 MeV/u for $\frac{d\sigma(\mathscr{E},0^\circ)}{d\Omega_{\mathrm{c.m.}}}$ and up to 100 MeV/u for the total cross section, whereas Legendre coefficients are tabulated up to 20 MeV/u as in Ref. [34].

Least squares approximations for both ^{2}H(d,n)^{3}He and ^{2}H(d,p)^{3}H reactions presented below were obtained using the data from works [50,52–95]. Experimental total cross sections are given in Refs. [52–56] at ultra-low energies under 10 keV/u, where they are expected to be governed predominantly by Gamow's theory. Experimental total cross sections at energies up to about 50 keV/u are shown in publications [57,58] and those at high energies around 20 MeV/u are shown in Ref. [59].

The rest of the mentioned data sources contain experimental differential cross sections except [64], where some theoretical predictions are given for ultra-high energy region around 600 MeV/u. The works [58,59,75–95] contain data for both neutron and proton reaction branches. The publications [50,52–54,60–64] cover only ^{2}H(d,n)^{3}He branch and the works [55–57,65–74] contain the data only for ^{2}H(d,p)^{3}H branch.

In Refs. [50,60–63,66–68,89–95] Legendre coefficients are used similarly to Eq. (1), while in [71–84] the authors deal with expansions in terms of even powers of $\cos\vartheta$, so a rearrangement of this kind

$$\begin{aligned} &A + B\cos^2\vartheta + C\cos^4\vartheta + D\cos^6\vartheta + \cdots \\ &\quad = (A + \tfrac{1}{3}B + \tfrac{1}{5}C + \tfrac{1}{7}D + \cdots)P_0(\cos\vartheta) + \cdots \\ &\qquad + (\tfrac{16}{231}D + \cdots)P_6(\cos\vartheta) + \cdots \end{aligned} \tag{5}$$

is required.

In Ref. [59] the incident deuteron momentum p_i in (MeV/c) is used to characterize collisions instead of the kinetic energy. From

the energy–momentum relation the total energy in (MeV) of the incident deuteron in the target frame is then

$$E_i = \sqrt{p_i^2 + m_d^2}, \tag{6}$$

where m_d is the deuteron rest mass in (MeV). The corresponding kinetic energy of the incident deuteron is

$$K_i = E_i - m_d. \tag{7}$$

In work [88] differential cross sections are expressed via Mandelstam variables s, the square of the invariant mass, and t, the square of the four-momentum transfer. In the target frame the total energy of the target deuteron equals m_d and its momentum is zero. Thus, the square of the total energy in the center of momentum frame, i.e. the square of the invariant mass, is

$$s = (E_i + m_d)^2 - p_i^2, \tag{8}$$

or, using Eq. (6),

$$s = 2m_d(E_i + m_d). \tag{9}$$

With m_1 and m_2 being the neutron mass and the helion mass, respectively, both in (MeV), for ^{2}H(d,n)^{3}He branch, or with m_1 and m_2 being the proton mass and the triton mass, respectively, both in (MeV), for ^{2}H(d,p)^{3}H branch, the relationship between the cosine of the polar angle in the center of momentum frame and the four-momentum transfer variable can be calculated as

$$\cos\vartheta = \frac{s^2 + s(2t - 2m_d^2 - m_1^2 - m_2^2)}{\sqrt{\lambda(s, m_d^2, m_d^2)\lambda(s, m_1^2, m_2^2)}}. \tag{10}$$

The relationship between $\frac{d\sigma}{dt}$ given in [88] and $\frac{d\sigma(\mathscr{E},\vartheta)}{d\Omega_{\text{c.m.}}}$ is established by the formula

$$dt = \frac{\sqrt{\lambda(s, m_d^2, m_d^2)\lambda(s, m_1^2, m_2^2)}}{4\pi s} d\Omega_{\text{c.m.}}. \tag{11}$$

The definition of the kinematic function λ, which appears in Eqs. (10) and (11), is

$$\lambda(x, y, z) = (x - y - z)^2 - 4yz. \tag{12}$$

Detailed derivations of the above formulae may be found in [96].

In Ref. [64] the energy range is comparable with work [88], however, recalculation according to Eq. (6) through Eq. (12) is not required because kinetic energies of deuterons are used, and differential cross sections are given in terms of the center of mass solid angle.

3. Parametrizations of total cross sections and astrophysical S-factors

Let us designate the specific Gamow energy for the interaction of two deuterons

$$\mathscr{E}_G = 2m_u c^2(\pi\alpha)^2, \tag{13}$$

where m_u is the unified atomic mass unit, c is the speed of light in vacuum, and α is the fine-structure constant. Up to date values of fundamental physical constants were published in work [97]. The specific astrophysical S-factor is

$$S(\mathscr{E}) = \mathscr{E}\sigma(\mathscr{E})\exp(\sqrt{\mathscr{E}_G/\mathscr{E}}). \tag{14}$$

To obtain traditional E_G (eV) and $S(E_{\text{c.m.}})$ (mb × eV), the values $\mathscr{E}_G$ (eV/u) and $\mathscr{E}$ (eV/u) in Eq. (13) and in Eq. (14) need to be multiplied by the reduced mass of two deuterons, expressed in unified atomic mass units.

Let us next introduce a nonlinear change of variable

$$\xi_j = 2\left(\frac{\ln\mathscr{E} - \ln\mathscr{E}_j^L}{\ln\mathscr{E}_j^U - \ln\mathscr{E}_j^L}\right) - 1, \tag{15}$$

where $\mathscr{E}_j^L$ and $\mathscr{E}_j^U$ are the lower end and the upper end of the specific energy range in which the parametrization is defined for the corresponding quantity. The subscript j is to distinguish between parameters pertaining to different quantities. Hereinafter, $j = -3$ corresponds to total cross sections, $j = -2$ corresponds to astrophysical S-factors, $j = -1$ corresponds to differential cross sections at 0°. The range $j = 0, \ldots, 8$ corresponds to normalized Legendre coefficients $a_{2j}(\mathscr{E})$.

The formulae to calculate the total cross section and the astrophysical S-factor are similar

$$\sigma(\mathscr{E}) = \exp\left(\sum_{k=0}^{15} b_{k,-3}T_k(\xi_{-3})\right), \tag{16}$$

$$S(\mathscr{E}) = \exp\left(\sum_{k=0}^{15} b_{k,-2}T_k(\xi_{-2})\right), \tag{17}$$

where $T_k(\xi_j)$ are Chebyshev polynomials of the first kind. Certainly, a parametrization of one of these quantities, $\sigma(\mathscr{E})$ or $S(\mathscr{E})$, is enough since the other one can be calculated using Eq. (14). However, both parametrizations are given for convenience.

Parameters $\mathscr{E}_j^L$ and $\mathscr{E}_j^U$ and Chebyshev coefficients $b_{k,j}$ to calculate the total cross sections and the astrophysical S-factors for ^{2}H(d,n)^{3}He and ^{2}H(d,p)^{3}H reactions are listed in Table 1 and in Table 3 respectively. Graph 1 shows the total cross section for ^{2}H(d,n)^{3}He reaction together with data points from the original bibliographic sources described in Section 2. Total cross section according to work [35] is also shown. Graph 2 shows the astrophysical S-factor for ^{2}H(d,n)^{3}He reaction together with data points and the approximation from Ref. [36] applicable in a narrower energy range. The total cross section and the astrophysical S-factor for ^{2}H(d,p)^{3}H reaction together with the original data points are shown in Graph 13 and Graph 14. The approximation of the astrophysical S-factor in a narrower energy range from Ref. [36] is also depicted. A comparison of the total cross sections calculated using Eq. (16) for the neutron branch and the proton branch is shown in Graph 23. Graph 24 shows a comparison of the astrophysical S-factors calculated using Eq. (17) for the two branches of the reaction.

4. Parametrizations of differential cross sections

The formula to calculate the differential cross section at 0° is analogous to Eqs. (16) and (17)

$$\frac{d\sigma(\mathscr{E}, 0°)}{d\Omega_{\text{c.m.}}} = \exp\left(\sum_{k=0}^{15} b_{k,-1}T_k(\xi_{-1})\right). \tag{18}$$

Parameters $\mathscr{E}_{-1}^L$ and $\mathscr{E}_{-1}^U$ and Chebyshev coefficients $b_{k,-1}$ for ^{2}H(d,n)^{3}He and ^{2}H(d,p)^{3}H reactions are listed in Table 1 and in Table 3 respectively. Graph 3 shows the differential cross section at 0° for ^{2}H(d,n)^{3}He reaction together with data points from the bibliographic sources. $\frac{d\sigma(\mathscr{E},0°)}{d\Omega_{\text{c.m.}}}$ according to work [35] is also shown. The differential cross section at 0° for ^{2}H(d,p)^{3}H reaction together with the original data points is shown in Graph 15. A comparison of the curves $\frac{d\sigma(\mathscr{E},0°)}{d\Omega_{\text{c.m.}}}$ calculated using Eq. (18) for the neutron branch and the proton branch is shown in Graph 25.

Normalized Legendre coefficients are calculated using a similar Chebyshev polynomial approximation, but in linear scale

$$a_{2j}(\mathscr{E}) = \sum_{k=0}^{15} b_{k,j}T_k(\xi_j), \tag{19}$$

where $j = 0, \ldots, 8$. Parameters $\mathscr{E}_j^L$ and $\mathscr{E}_j^U$, needed to apply the variable change Eq. (15), and Chebyshev coefficients $b_{k,j}$ are listed in Table 2 for ^{2}H(d,n)^{3}He reaction and in Table 4 for ^{2}H(d,p)^{3}H reaction. Graphs 4–12 depict the normalized Legendre coefficients $a_0(\mathscr{E})$ - $a_{16}(\mathscr{E})$ calculated using Eq. (19) for ^{2}H(d,n)^{3}He reaction together with bibliographic data points and curves from [35]. Our parametrizations of $a_0(\mathscr{E})$ and $a_2(\mathscr{E})$ below 6 keV/u, where no data points are available, merely represent extrapolations. The behavior of $\frac{d\sigma(\mathscr{E},0^\circ)}{d\Omega_{\mathrm{c.m.}}}$ in the ultra-low energy region is governed by the behavior of the total cross section and the relationship established by Eq. (4). Normalized Legendre coefficients $a_0(\mathscr{E})$ - $a_{12}(\mathscr{E})$ calculated using Eq. (19) for ^{2}H(d,p)^{3}H reaction and the data points from bibliography are shown in Graphs 16–22. Again, in the energy region below 6 keV/u parametrizations of $a_0(\mathscr{E})$ and $a_2(\mathscr{E})$ represent extrapolations. Higher order normalized Legendre coefficients $a_{14}(\mathscr{E})$ and $a_{16}(\mathscr{E})$ contribute at high energies. These coefficients are the same as for ^{2}H(d,n)^{3}He reaction. The same set of data points from [64,85–88] was used due to charge symmetry in the high energy range according to Refs. [85,87]. The data above 10 MeV/u are scarce in literature, thus further amendments of the parametrizations may be needed in the high energy range.

Graph 26 shows a comparison between normalized Legendre coefficients $a_0(\mathscr{E})$–$a_{12}(\mathscr{E})$ calculated using Eq. (19) for the neutron and the proton branch of the reaction. Noticeable differences can be seen, which are larger for lower order coefficients and smaller for higher order coefficients. The greater coefficient alternates, i.e. $a_0(\mathscr{E})$ is greater for the proton branch, $a_2(\mathscr{E})$ is greater for the neutron branch, and so on.

Differential cross sections are calculated in accordance with Eq. (3). The series is truncated at $L = 8$ inclusively, analogously to works [33–35]. The upper end of the specific energy range $\mathscr{E}_j^U$ is the same for all Legendre coefficients $a_{2j}(\mathscr{E})$ with $j = 0, \ldots, 8$, but the lower ends $\mathscr{E}_j^L$ are different, monotonously increasing with index j. Therefore, with

$$\mathrm{sign}(x) = \begin{cases} -1, & x < 0 \\ 1 & x \geqslant 0 \end{cases} \tag{20}$$

the actual index L of the highest order Legendre coefficient with a nonzero contribution at a given specific energy $\mathscr{E}$ can be calculated as

$$L = \sum_{j=1}^{8} \frac{\mathrm{sign}(\mathscr{E} - \mathscr{E}_j^L) + 1}{2}. \tag{21}$$

Surface plots of differential cross sections calculated using Eqs. (3) and (18)–(21) for both the neutron and the proton branch of the reaction are shown in Graph 27.

5. Summary

New parametrizations for center of mass differential cross sections of deuteron–deuteron fusion reactions in a wide range of specific energy from 0.5 keV/u to about 0.5 GeV/u have been obtained. In the earlier bibliography neither systemized collections of differential cross section data, nor compact parametrizations for ^{2}H(d,p)^{3}H reaction were available, whilst experimental results are as abundant as for ^{2}H(d,n)^{3}He reaction. For the neutron production reaction ^{2}H(d,n)^{3}He previously available recommended differential cross sections were in the form of tables implying the need for search and interpolation.

Straightforward approximating formulae are given here for both the neutron and the proton branch of the reaction. The energy range is about two orders of magnitude broader than that in the tables published earlier. Parametrizations for total cross sections and astrophysical S-factors are also given. All the formulae are readily suitable for multithreaded algorithmization. These results may be used primarily in astrophysics, high energy physics, and controlled nuclear fusion research.

References

[1] A. Coc, et al., Astrophys. J. 744 (2012) 158.
[2] A. Coc, J. Phys.: Conf. Ser. 665 (2016) 012001.
[3] R.G. Pizzone, et al., Astrophys. J. 786 (2014) 112.
[4] A. Tumino, et al., Astrophys. J. 785 (2014) 96.
[5] C. Angulo, P. Descouvemont, Nuclear Phys. A 639 (1998) 733.
[6] P. Descouvemont, At. Data Nucl. Data Tables 88 (2004) 203.
[7] C. Li, et al., Phys. Rev. C 92 (2015) 025805.
[8] A. Tumino, et al., J. Phys.: Conf. Ser. 665 (2016) 012009.
[9] G.S. Chulick, et al., Nuclear Phys. A 551 (1993) 255.
[10] D.U.L. Yu, Progr. Theoret. Phys. 36 (1966) 734.
[11] S. Barshay, G.M. Temmer, Phys. Rev. Lett. 12 (1964) 728.
[12] W.C. Haxton, E.M. Henley (Eds.), Symmetries and Fundamental Interactions in Nuclei, World Scientific Publishing, Singapore, 1995, p. 127.
[13] V. König, et al., Phys. Lett. B 72 (1978) 436.
[14] V. König, et al., Nuclear Phys. A 331 (1979) 1.
[15] F. Nebia, et al., C. R. Phys. 3 (2002) 733.
[16] E.A. Azizov, et al., Phys. Atom. Nucl. 79 (2016) 1125.
[17] B.V. Kuteev, et al., Nucl. Fusion 55 (2015) 073035.
[18] Yu.E. Titarenko, et al., At. Energ. 120 (2016) 55.
[19] A.V. Zhirkin, et al., Nucl. Fusion 55 (2015) 113007.
[20] L. Jia, et al., Plasma Sci. Technol. 18 (2016) 179.
[21] A.M. Garofalo, et al., Fusion Eng. Des. 89 (2014) 876.
[22] V.S. Chan, et al., Nucl. Fusion 55 (2015) 023017.
[23] B.N. Sorbom, et al., Fusion Eng. Des. 100 (2015) 378.
[24] M. Tardocchi, et al., Plasma Phys. Control. Fusion 55 (2013) 074014.
[25] F. Moro, et al., Fusion Eng. Des. (2017). http://dx.doi.org/10.1016/j.fusengdes.2017.01.031, in press.
[26] D. Funaki, et al., Rev. Sci. Instrum. 79 (2008) 10E512.
[27] M. Garcia-Muñoz, et al., Rev. Sci. Instrum. 87 (2016) 11D829.
[28] G.J. Wilkie, et al., Phys. Plasmas 23 (2016) 060703.
[29] M.F. Hawthorne, et al. (Eds.), Frontiers in Neutron Capture Therapy, Springer Science+Business Media, New York, 2001, p. 483.
[30] E. Durisi, et al., Nucl. Instrum. Methods Phys. Res. A 574 (2007) 363.
[31] S. Savolainen, et al., Phys. Medica 29 (2013) 233.
[32] H. Liskien, A. Paulsen, Nucl. Data Tables 11 (1973) 569.
[33] M. Drosg, O. Schwerer, IAEA Technical Reports Series No. 273 STI/DOC/10/273, 1987, p. 83.
[34] M. Drosg, Report IAEA-NDS-87 Rev. 9, IAEA Nuclear Data Section, 2005.
[35] M. Drosg, N. Otuka, IAEA Report INDC(AUS)-0019, 2015.
[36] H.-S. Bosch, G.M. Hale, Nucl. Fusion 32 (1992) 611.
[37] E.J. Konopinski, E. Teller, Phys. Rev. 73 (1948) 822.
[38] F.M. Beiduk, et al., Phys. Rev. 77 (1950) 622.
[39] J.R. Pruett, et al., Phys. Rev. 77 (1950) 628.
[40] W.M. Fairbairn, Proc. Phys. Soc. A 67 (1954) 990.
[41] N.B. Ladygina, Few-Body Syst. 53 (2012) 253.
[42] A. Deltuva, A.C. Fonseca, Phys. Rev. C 76 (2007) 021001(R).
[43] A. Deltuva, A.C. Fonseca, Phys. Rev. C 95 (2017) 024003.
[44] P. Grassberger, W. Sandhas, Nuclear Phys. B 2 (1967) 181.
[45] L.D. Faddeev, Sov. Phys. JETP 12 (1961) 1014.
[46] Yu.N. Uzikov, JETP Lett. 81 (2005) 303.
[47] H. Paetz gen. Schieck, Eur. Phys. J. A 44 (2010) 321.
[48] G. Ciullo, et al. (Eds.), Nuclear Fusion with Polarized Fuel, in: Springer Proceedings in Physics, vol. 187, Springer International Publishing, Switzerland, 2016, p. 15.
[49] M. Drosg, Nucl. Sci. Eng. 67 (1978) 190.
[50] M. Drosg, Los Alamos Scientific Laboratory Report LA-8538, 1980.
[51] R.W. Fegley, (Ph.D. thesis), University of California, Davis, 1970.
[52] V.M. Bystritskiĭ, et al., Phys. Atom. Nuclei 64 (2001) 855.
[53] V.M. Bystritsky, et al., Phys. Atom. Nuclei 66 (2003) 1683.
[54] V.M. Bystritsky, et al., Eur. Phys. J. A 36 (2008) 151.
[55] A. von Engel, C.C. Goodyear, Proc. R. Soc. Lond. Ser. A Math. Phys. Eng. Sci. 264 (1961) 445.
[56] D. Magnac-Valette, et al., J. Phys. Radium 21 (1960) 125.
[57] C.F. Cook, J.R. Smith, Phys. Rev. 89 (1953) 785.
[58] W.R. Arnold, et al., Phys. Rev. 93 (1954) 483.
[59] J.E.A. Lys, L. Lyons, Nuclear Phys. 74 (1965) 261.
[60] W.W. Daehnick, J.M. Fowler, Phys. Rev. 111 (1958) 1309.
[61] M.D. Goldberg, J.M. Le Blanc, Phys. Rev. 119 (1960) 1992.
[62] S.T. Thornton, Nuclear Phys. A 136 (1969) 25.
[63] A.B. Jones, Aust. J. Phys. 33 (1980) 203.
[64] C. Wilkin, J. Phys. G: Nucl. Phys. 6 (1980) 69.
[65] C.S. Godfrey, Phys. Rev. 96 (1954) 493.
[66] H.B. Burrows, et al., Proc. R. Soc. Lond. Ser. A Math. Phys. Eng. Sci. 209 (1951) 489.
[67] J.C. Allred, et al., Phys. Rev. 82 (1951) 782.
[68] W.A. Wenzel, W. Whaling, Phys. Rev. 88 (1952) 1149.
[69] W. Grüebler, et al., Nuclear Phys. A 193 (1972) 129.
[70] W. Grüebler, et al., Nuclear Phys. A 369 (1981) 381.

[71] P.A. Davenport, et al., Proc. R. Soc. Lond. Ser. A Math. Phys. Eng. Sci. 216 (1953) 66.
[72] J. Moffatt, et al., Proc. R. Soc. Lond. Ser. A Math. Phys. Eng. Sci. 212 (1952) 220.
[73] H.A. Leiter, et al., Phys. Rev. 78 (1950) 663.
[74] E. Bretscher, et al., Phys. Rev. 73 (1948) 815.
[75] E.A. Eliot, et al., Proc. R. Soc. Lond. Ser. A Math. Phys. Eng. Sci. 216 (1953) 57.
[76] R.B. Theus, et al., Nuclear Phys. 80 (1966) 273.
[77] R.E. Brown, N. Jarmie, Phys. Rev. C 41 (1990) 1391.
[78] D.L. Booth, et al., Proc. Phys. Soc. A 69 (1956) 265.
[79] G. Preston, et al., Proc. R. Soc. Lond. Ser. A Math. Phys. Eng. Sci. 226 (1954) 206.
[80] A.S. Ganeev, et al., Sov. J. At. Energ. Suppl. 5 (1957) 26 (in Russian).
[81] V.V. Volkov, et al., Sov. J. At. Energ. Suppl. 5 (1957) 15 (in Russian).
[82] J.M. Blair, et al., Phys. Rev. 74 (1948) 1599.
[83] K.G. McNeill, G.M. Keyser, Phys. Rev. 81 (1951) 602.
[84] N. Ying, et al., Nuclear Phys. A 206 (1973) 481.
[85] M. Roy, et al., Phys. Lett. B 29 (1969) 95.
[86] C. Alderliesten, et al., Phys. Rev. C 18 (1978) 2001.
[87] H. Brückmann, et al., Z. Phys. 230 (1970) 383.
[88] G. Bizard, et al., Phys. Rev. C 22 (1980) 1632.
[89] A. Krauss, et al., Nuclear Phys. A 465 (1987) 150.
[90] R.L. Schulte, et al., Nuclear Phys. A 192 (1972) 609.
[91] J.E. Brolley, et al., Phys. Rev. 107 (1957) 820.
[92] W.T.H. Van Oers, K.W. Brockman, Nuclear Phys. 48 (1963) 625.
[93] A. Okihana, et al., J. Phys. Soc. Japan 46 (1979) 707.
[94] U. Greife, et al., Z. Phys. A 351 (1995) 107.
[95] D.S. Leonard, et al., Phys. Rev. C 73 (2006) 045801.
[96] E. Byckling, K. Kajantie, Particle Kinematics, John Wiley and Sons, London, 1973, p. 76.
[97] P.J. Mohr, et al., Rev. Modern Phys. 88 (2016) 035009.

Explanation of Tables

The subscript j is used to distinguish between parameters pertaining to different quantities. In Tables 1 and 3 the columns for $j = -3$ correspond to total cross sections, the columns for $j = -2$ correspond to astrophysical S-factors, and the columns for $j = -1$ correspond to 0° differential cross sections. In Tables 2 and 4 the columns for the range $j = 0, \ldots, 8$ correspond to normalized Legendre coefficients $a_{2j}(\mathscr{E})$.

Table 1. **Chebyshev coefficients $b_{k,j}$ for $k = 0, \ldots, 15, j = -3, -2, -1$ and lower $\mathscr{E}_j^L$ and upper $\mathscr{E}_j^U$ ends of the specific energy range for total cross section $\sigma(\mathscr{E})$, astrophysical factor $S(\mathscr{E})$ and the 0° c.m. differential cross section $\frac{d\sigma(\mathscr{E},0°)}{d\Omega_{\text{c.m.}}}$ for ^{2}H(d,n)^{3}He reaction.**
To calculate the total cross section, Eq. (16) should be used. To calculate the astrophysical S-factor, Eq. (17) should be used. For the differential cross section at 0° a similar expression is given by Eq. (18). For the nonlinear variable change apply Eq. (15) with $\mathscr{E}_j^L$ and $\mathscr{E}_j^U$ from the appropriate column of the table.

Table 2. **Chebyshev coefficients $b_{k,j}$ for $k = 0, \ldots, 15, j = 0, \ldots, 8$ and lower $\mathscr{E}_j^L$ and upper $\mathscr{E}_j^U$ ends of the specific energy range for normalized Legendre coefficients $a_{2j}(\mathscr{E})$ for ^{2}H(d,n)^{3}He reaction.**
The differential cross section is calculated according to Eqs. (3), (18), and (19) as

$$\frac{d\sigma(\mathscr{E},\vartheta)}{d\Omega_{\text{c.m.}}} = \frac{d\sigma(\mathscr{E},0°)}{d\Omega_{\text{c.m.}}} \sum_{j=0}^{L} \left(\sum_{k=0}^{15} b_{k,j} T_k(\xi_j) \right) P_{2j}(\cos\vartheta)$$

with the upper limit of the summation L given by Eq. (21). For the nonlinear variable change apply Eq. (15) with $\mathscr{E}_j^L$ and $\mathscr{E}_j^U$ from the appropriate column of the table.

Table 3. **Chebyshev coefficients $b_{k,j}$ for $k = 0, \ldots, 15, j = -3, -2, -1$ and lower $\mathscr{E}_j^L$ and upper $\mathscr{E}_j^U$ ends of the specific energy range for total cross section $\sigma(\mathscr{E})$, astrophysical factor $S(\mathscr{E})$ and the 0° c.m. differential cross section $\frac{d\sigma(\mathscr{E},0°)}{d\Omega_{\text{c.m.}}}$ for ^{2}H(d,p)^{3}H reaction.**
The total cross section, the astrophysical S-factor, and the differential cross section at 0° are calculated similarly to the explanation of Table 1.

Table 4. **Chebyshev coefficients $b_{k,j}$ for $k = 0, \ldots, 15, j = 0, \ldots, 8$ and lower $\mathscr{E}_j^L$ and upper $\mathscr{E}_j^U$ ends of the specific energy range for normalized Legendre coefficients $a_{2j}(\mathscr{E})$ for ^{2}H(d,p)^{3}H reaction.**
The differential cross section is calculated similarly to the explanation of Table 2.

Explanation of Graphs

Graph 1. **Total cross section of ^{2}H(d,n)^{3}He reaction.**
Graph 2. **Astrophysical S-factor for ^{2}H(d,n)^{3}He reaction.**
Graph 3. **Differential cross section at 0° in the c.m. frame $\frac{d\sigma(\mathscr{E},0°)}{d\Omega_{\text{c.m.}}}$ for ^{2}H(d,n)^{3}He reaction.**
Graph 4. **Normalized Legendre coefficient a_0 for ^{2}H(d,n)^{3}He reaction.**
Graph 5. **Normalized Legendre coefficient a_2 for ^{2}H(d,n)^{3}He reaction.**
Graph 6. **Normalized Legendre coefficient a_4 for ^{2}H(d,n)^{3}He reaction.**
Graph 7. **Normalized Legendre coefficient a_6 for ^{2}H(d,n)^{3}He reaction.**
Graph 8. **Normalized Legendre coefficient a_8 for ^{2}H(d,n)^{3}He reaction.**
Graph 9. **Normalized Legendre coefficient a_{10} for ^{2}H(d,n)^{3}He reaction.**
Graph 10. **Normalized Legendre coefficient a_{12} for ^{2}H(d,n)^{3}He reaction.**
Graph 11. **Normalized Legendre coefficient a_{14} for ^{2}H(d,n)^{3}He and ^{2}H(d,p)^{3}H reactions.**
Graph 12. **Normalized Legendre coefficient a_{16} for ^{2}H(d,n)^{3}He and ^{2}H(d,p)^{3}H reactions.**
Graph 13. **Total cross section of ^{2}H(d,p)^{3}H reaction.**
Graph 14. **Astrophysical S-factor for ^{2}H(d,p)^{3}H reaction.**
Graph 15. **Differential cross section at 0° in the c.m. frame $\frac{d\sigma(\mathscr{E},0°)}{d\Omega_{\text{c.m.}}}$ for ^{2}H(d,p)^{3}H reaction.**
Graph 16. **Normalized Legendre coefficient a_0 for ^{2}H(d,p)^{3}H reaction.**
Graph 17. **Normalized Legendre coefficient a_2 for ^{2}H(d,p)^{3}H reaction.**
Graph 18. **Normalized Legendre coefficient a_4 for ^{2}H(d,p)^{3}H reaction.**
Graph 19. **Normalized Legendre coefficient a_6 for ^{2}H(d,p)^{3}H reaction.**
Graph 20. **Normalized Legendre coefficient a_8 for ^{2}H(d,p)^{3}H reaction.**
Graph 21. **Normalized Legendre coefficient a_{10} for ^{2}H(d,p)^{3}H reaction.**
Graph 22. **Normalized Legendre coefficient a_{12} for ^{2}H(d,p)^{3}H reaction.**
Graph 23. **Total cross sections of ^{2}H(d,n)^{3}He (black dashed curve) and ^{2}H(d,p)^{3}H (gray solid curve) reactions calculated using Chebyshev coefficients from Tables 1 and 3 correspondingly.**
Graph 24. **Astrophysical S-factors for ^{2}H(d,n)^{3}He (black dashed curve) and ^{2}H(d,p)^{3}H (gray solid curve) reactions calculated using Chebyshev coefficients from Tables 1 and 3 correspondingly.**
Graph 25. **Differential cross sections at 0° in the c.m. frame $\frac{d\sigma(\mathscr{E},0°)}{d\Omega_{\text{c.m.}}}$ for ^{2}H(d,n)^{3}He (black dashed curve) and ^{2}H(d,p)^{3}H (gray solid curve) reactions calculated using Chebyshev coefficients from Tables 1 and 3 correspondingly.**
Graph 26. **Normalized Legendre coefficients a_{2j} for $j = 0, \ldots, 6$ for ^{2}H(d,n)^{3}He (black dashed curves) and ^{2}H(d,p)^{3}H (gray solid curves) reactions calculated using Chebyshev coefficients from Tables 2 and 4 correspondingly.**
Graph 27. **Differential cross sections in the c.m. frame for ^{2}H(d,n)^{3}He (black mesh) and ^{2}H(d,p)^{3}H (gray surface) reactions calculated using Chebyshev coefficients from Tables 1–4**

The correspondence of references in Graphs 1–22 to the list of bibliographic references after the text is by the family name of the first author.
Bystritsky corresponds to Refs. [52–54].
Drosg corresponds to Ref. [50].
Drosg (INDC(AUS)-0019) corresponds to Ref. [35].

Table 1
Chebyshev coefficients $b_{k,j}$ for $k = 0, \ldots, 15$, $j = -3, -2, -1$ and lower $\mathscr{E}_j^L$ and upper $\mathscr{E}_j^U$ ends of the specific energy range for total cross section $\sigma(\mathscr{E})$, astrophysical factor $S(\mathscr{E})$ and the 0° c.m. differential cross section $\frac{d\sigma(\mathscr{E},0^\circ)}{d\Omega_{\mathrm{c.m.}}}$ for ^{2}H(d,n)^{3}He reaction.

	$j = -3$ for $\sigma(\mathscr{E})$	$j = -2$ for $S(\mathscr{E})$	$j = -1$ for $\frac{d\sigma(\mathscr{E},0^\circ)}{d\Omega_{\mathrm{c.m.}}}$
$\mathscr{E}_j^L$ (eV/u)	0.5000E+03	0.5000E+03	0.5000E+03
$\mathscr{E}_j^U$ (eV/u)	0.6357E+09	0.6357E+09	0.6357E+09
$b_{0,j}$	−0.5007E+01	0.1808E+02	−0.6216E+01
$b_{1,j}$	0.9208E+01	−0.3366E+00	0.1086E+02
$b_{2,j}$	−0.1176E+02	−0.1509E+01	−0.1154E+02
$b_{3,j}$	0.3588E+01	−0.1314E+01	0.3408E+01
$b_{4,j}$	−0.2234E+01	−0.3464E+00	−0.2287E+01
$b_{5,j}$	0.7525E+00	0.1484E+00	0.8509E+00
$b_{6,j}$	−0.5853E−01	0.1053E+00	0.4642E−01
$b_{7,j}$	0.3849E−01	0.1429E−02	0.7690E−01
$b_{8,j}$	−0.4203E−01	−0.3549E−01	−0.3457E−01
$b_{9,j}$	−0.5261E−01	−0.5316E−01	−0.2966E−01
$b_{10,j}$	−0.2706E−01	−0.2647E−01	−0.2997E−02
$b_{11,j}$	0.1934E−01	0.1836E−01	0.1617E−01
$b_{12,j}$	0.1936E−01	0.2088E−01	−0.6876E−03
$b_{13,j}$	−0.2310E−02	−0.3240E−02	−0.6203E−02
$b_{14,j}$	−0.1739E−01	−0.1681E−01	−0.2542E−02
$b_{15,j}$	−0.1391E−01	−0.1330E−01	−0.1209E−02

Table 2
Chebyshev coefficients $b_{k,j}$ for $k = 0, \ldots, 15$, $j = 0, \ldots, 8$ and lower $\mathscr{E}_j^L$ and upper $\mathscr{E}_j^U$ ends of the specific energy range for normalized Legendre coefficients $a_{2j}(\mathscr{E})$ for ^{2}H(d,n)^{3}He reaction.

	$j = 0$ for $a_0(\mathscr{E})$	$j = 1$ for $a_2(\mathscr{E})$	$j = 2$ for $a_4(\mathscr{E})$	$j = 3$ for $a_6(\mathscr{E})$	$j = 4$ for $a_8(\mathscr{E})$	$j = 5$ for $a_{10}(\mathscr{E})$	$j = 6$ for $a_{12}(\mathscr{E})$	$j = 7$ for $a_{14}(\mathscr{E})$	$j = 8$ for $a_{16}(\mathscr{E})$
$\mathscr{E}_j^L$ (eV/u)	0.5000E+03	0.5000E+03	0.1500E+05	0.5000E+06	0.1500E+07	0.3000E+07	0.3500E+07	0.4000E+07	0.7000E+07
$\mathscr{E}_j^U$ (eV/u)	0.6357E+09	0.6357E+09	0.6357E+09	0.6357E+09	0.6357E+09	0.6357E+09	0.6357E+09	0.6357E+09	0.6357E+09
$b_{0,j}$	0.4648E+00	0.1874E+00	0.1510E+00	0.1590E+00	0.1079E+00	0.6604E−01	0.3578E−01	0.1907E−01	0.7836E−02
$b_{1,j}$	−0.5290E+00	0.5640E−01	0.1201E+00	0.1023E+00	0.7303E−01	0.4495E−01	0.2848E−01	0.1387E−01	0.2576E−02
$b_{2,j}$	0.7126E−01	−0.1354E+00	−0.6595E−01	−0.7163E−01	−0.4843E−01	−0.2997E−01	−0.1559E−01	−0.9393E−02	−0.6040E−02
$b_{3,j}$	0.6804E−01	0.5168E−01	0.8920E−02	0.2931E−01	0.1289E−01	0.6940E−02	−0.2888E−02	−0.2736E−02	−0.3687E−03
$b_{4,j}$	−0.1003E−01	0.4814E−01	0.6132E−01	0.3931E−01	0.3902E−01	0.3191E−01	0.1733E−01	0.8071E−02	0.4008E−02
$b_{5,j}$	−0.2357E−01	−0.3992E−01	−0.2995E−01	−0.2070E−01	0.1345E−01	0.1919E−01	0.1717E−01	0.9220E−02	0.2419E−02
$b_{6,j}$	−0.7292E−02	−0.4426E−01	−0.7179E−01	−0.1986E−01	−0.5551E−02	0.8264E−03	0.3697E−02	−0.1110E−04	−0.2283E−02
$b_{7,j}$	0.5925E−02	−0.6700E−02	−0.9176E−02	−0.6215E−02	−0.9883E−02	−0.4302E−02	−0.1845E−02	−0.2245E−02	0.8274E−03
$b_{8,j}$	0.3205E−02	0.1234E−02	0.1943E−01	−0.1132E−02	−0.4587E−02	−0.2261E−02	0.1309E−02	0.2802E−02	0.3053E−02
$b_{9,j}$	−0.4462E−02	−0.1077E−01	−0.1288E−02	−0.2584E−04	−0.5217E−03	−0.9494E−03	0.1262E−02	0.2687E−02	0.4117E−03
$b_{10,j}$	−0.5576E−02	−0.4571E−02	−0.8204E−03	−0.3724E−02	0.2393E−02	0.8136E−03	−0.2522E−03	−0.5903E−03	−0.2991E−03
$b_{11,j}$	0.2836E−02	0.8117E−02	0.9707E−02	−0.4313E−02	0.2766E−02	0.2237E−02	0.5265E−03	−0.5886E−03	0.4836E−04
$b_{12,j}$	0.4819E−02	0.8877E−02	0.4250E−02	−0.1196E−02	0.8592E−03	0.6114E−03	0.8053E−03	0.1091E−02	0.6702E−04
$b_{13,j}$	−0.1339E−02	0.1977E−02	−0.3891E−02	0.2419E−03	−0.8839E−03	−0.7011E−03	0.4272E−03	0.5611E−03	−0.1337E−04
$b_{14,j}$	−0.3076E−02	−0.1786E−02	−0.4215E−02	−0.8159E−03	−0.5295E−03	0.6212E−04	0.5165E−04	−0.2562E−03	−0.1014E−04
$b_{15,j}$	0.2735E−03	−0.1544E−02	−0.1448E−02	−0.9323E−03	0.2565E−03	0.1966E−03	−0.6204E−05	−0.1772E−04	0.9341E−04

Table 3
Chebyshev coefficients $b_{k,j}$ for $k = 0, \ldots, 15$, $j = -3, -2, -1$ and lower $\mathscr{E}_j^L$ and upper $\mathscr{E}_j^U$ ends of the specific energy range for total cross section $\sigma(\mathscr{E})$, astrophysical factor $S(\mathscr{E})$ and the 0° c.m. differential cross section $\frac{d\sigma(\mathscr{E},0^\circ)}{d\Omega_{\text{c.m.}}}$ for ^{2}H(d,p)^{3}H reaction.

	$j = -3$ for $\sigma(\mathscr{E})$	$j = -2$ for $S(\mathscr{E})$	$j = -1$ for $\frac{d\sigma(\mathscr{E},0^\circ)}{d\Omega_{\text{c.m.}}}$
$\mathscr{E}_j^L$ (eV/u)	0.5000E+03	0.5000E+03	0.5000E+03
$\mathscr{E}_j^U$ (eV/u)	0.6357E+09	0.6357E+09	0.6357E+09
$b_{0,j}$	−0.5035E+001	0.1805E+02	−0.6279E+01
$b_{1,j}$	0.9195E+001	−0.3403E+00	0.1087E+02
$b_{2,j}$	−0.1169E+002	−0.1440E+01	−0.1143E+02
$b_{3,j}$	0.3588E+001	−0.1310E+01	0.3383E+01
$b_{4,j}$	−0.2278E+001	−0.3926E+00	−0.2325E+01
$b_{5,j}$	0.7441E+000	0.1397E+00	0.8447E+00
$b_{6,j}$	−0.3896E−001	0.1265E+00	0.5799E−01
$b_{7,j}$	0.4047E−001	0.1030E−02	0.8133E−01
$b_{8,j}$	−0.4490E−001	−0.3658E−01	−0.2447E−01
$b_{9,j}$	−0.3190E−001	−0.3347E−01	−0.5487E−02
$b_{10,j}$	−0.2904E−001	−0.2877E−01	−0.1301E−01
$b_{11,j}$	−0.1444E−002	−0.1486E−02	−0.8248E−02
$b_{12,j}$	0.1439E−001	0.1440E−01	−0.1991E−03
$b_{13,j}$	−0.8158E−002	−0.8159E−02	−0.4650E−02
$b_{14,j}$	−0.1720E−001	−0.1720E−01	−0.1774E−04
$b_{15,j}$	−0.3933E−002	−0.3933E−02	0.7734E−02

Table 4
Chebyshev coefficients $b_{k,j}$ for $k = 0, \ldots, 15$, $j = 0, \ldots, 8$ and lower $\mathscr{E}_j^L$ and upper $\mathscr{E}_j^U$ ends of the specific energy range for normalized Legendre coefficients $a_{2j}(\mathscr{E})$ for ^{2}H(d,p)^{3}H reaction.

	$j = 0$ for $a_0(\mathscr{E})$	$j = 1$ for $a_2(\mathscr{E})$	$j = 2$ for $a_4(\mathscr{E})$	$j = 3$ for $a_6(\mathscr{E})$	$j = 4$ for $a_8(\mathscr{E})$	$j = 5$ for $a_{10}(\mathscr{E})$	$j = 6$ for $a_{12}(\mathscr{E})$	$j = 7$ for $a_{14}(\mathscr{E})$	$j = 8$ for $a_{16}(\mathscr{E})$
$\mathscr{E}_j^L$ (eV/u)	0.5000E+03	0.5000E+03	0.1500E+05	0.5000E+06	0.1500E+07	0.3000E+07	0.3500E+07	0.4000E+07	0.7000E+07
$\mathscr{E}_j^U$ (eV/u)	0.6357E+09	0.6357E+09	0.6357E+09	0.6357E+09	0.6357E+09	0.6357E+09	0.6357E+09	0.6357E+09	0.6357E+09
$b_{0,j}$	0.4884E+00	0.1622E+00	0.1545E+00	0.1579E+00	0.1079E+00	0.6600E−01	0.3578E−01	0.1907E−01	0.7836E−02
$b_{1,j}$	−0.5522E+00	0.8046E−01	0.1168E+00	0.1035E+00	0.7314E−01	0.4485E−01	0.2849E−01	0.1387E−01	0.2576E−02
$b_{2,j}$	0.5487E−01	−0.1158E+00	−0.6936E−01	−0.7040E−01	−0.4808E−01	−0.2995E−01	−0.1560E−01	−0.9393E−02	−0.6040E−02
$b_{3,j}$	0.9479E−01	0.2273E−01	0.1528E−01	0.2752E−01	0.1230E−01	0.6914E−02	−0.2877E−02	−0.2736E−02	−0.3687E−03
$b_{4,j}$	−0.2170E−01	0.5620E−01	0.5950E−01	0.4001E−01	0.3891E−01	0.3191E−01	0.1730E−01	0.8071E−02	0.4008E−02
$b_{5,j}$	−0.2656E−01	−0.3404E−01	−0.3337E−01	−0.1978E−01	0.1342E−01	0.1916E−01	0.1719E−01	0.9220E−02	0.2419E−02
$b_{6,j}$	−0.2180E−02	−0.4592E−01	−0.6803E−01	−0.2047E−01	−0.5637E−02	0.7476E−03	0.3656E−02	−0.1110E−04	−0.2283E−02
$b_{7,j}$	0.6378E−02	−0.1001E−01	−0.8946E−02	−0.6396E−02	−0.9631E−02	−0.4357E−02	−0.1820E−02	−0.2245E−02	0.8274E−03
$b_{8,j}$	0.5984E−04	0.1217E−02	0.1747E−01	−0.5983E−03	−0.4642E−02	−0.2222E−02	0.1275E−02	0.2802E−02	0.3053E−02
$b_{9,j}$	−0.5832E−02	−0.7302E−02	−0.1477E−03	0.3012E−03	−0.5450E−03	−0.1020E−02	0.1270E−02	0.2687E−02	0.4117E−03
$b_{10,j}$	−0.2360E−02	−0.5536E−02	−0.1950E−03	−0.3859E−02	0.2488E−02	0.7774E−03	−0.2598E−03	−0.5903E−03	−0.2991E−03
$b_{11,j}$	0.3253E−02	0.6403E−02	0.9222E−02	−0.4430E−02	0.2424E−02	0.2210E−02	0.4977E−03	−0.5886E−03	0.4836E−04
$b_{12,j}$	0.2672E−02	0.9520E−02	0.4324E−02	−0.1074E−02	0.1753E−03	0.4898E−03	0.8335E−03	0.1091E−02	0.6702E−04
$b_{13,j}$	−0.1690E−02	0.2823E−02	−0.3113E−02	0.9140E−03	−0.8922E−03	−0.6538E−03	0.3617E−03	0.5611E−03	−0.1337E−04
$b_{14,j}$	−0.2152E−02	−0.2167E−02	−0.3652E−02	−0.4582E−03	−0.8688E−03	0.1090E−03	0.1013E−03	−0.2562E−03	−0.1014E−04
$b_{15,j}$	−0.3726E−03	−0.1394E−02	−0.1373E−02	−0.1034E−02	−0.2068E−04	0.1632E−03	−0.8350E−04	−0.1772E−04	0.9341E−04

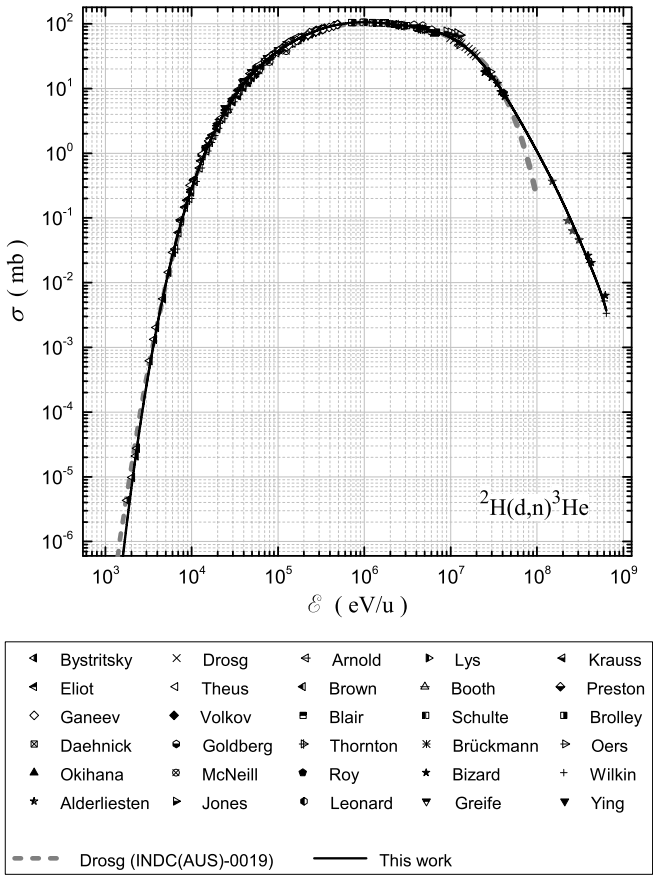

Graph 1. Total cross section of $^{2}H(d,n)^{3}He$ reaction.

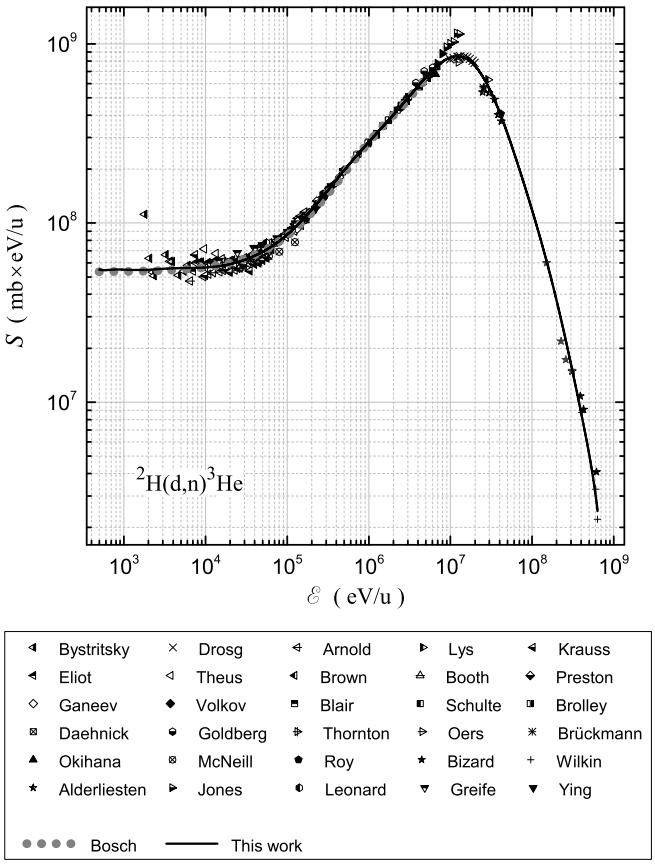

Graph 2. Astrophysical S-factor for ^{2}H(d,n)^{3}He reaction.

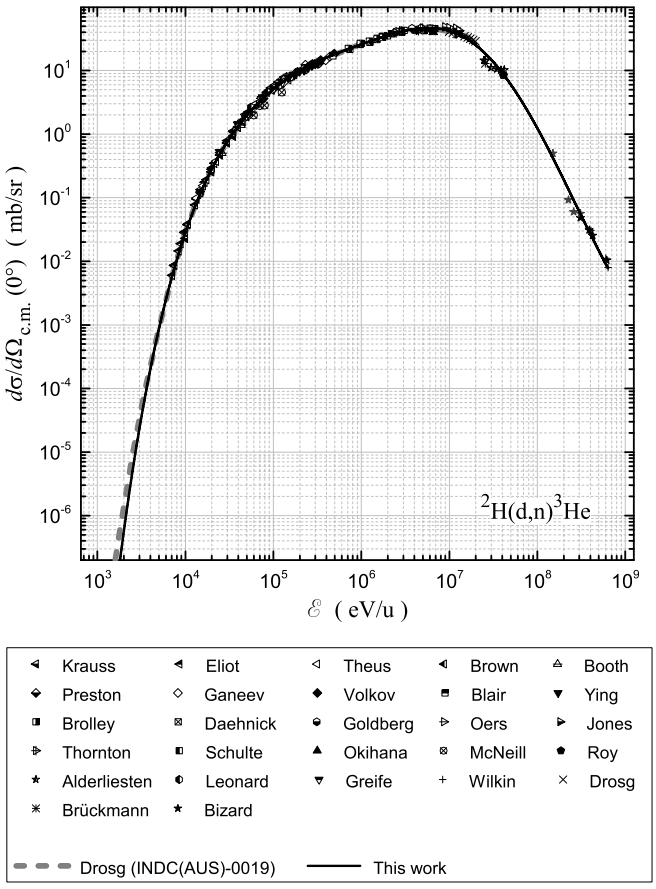

Graph 3. Differential cross section at 0° in the c.m. frame $\frac{d\sigma(\mathscr{E},0^\circ)}{d\Omega_{c.m.}}$ for ^{2}H(d,n)^{3}He reaction.

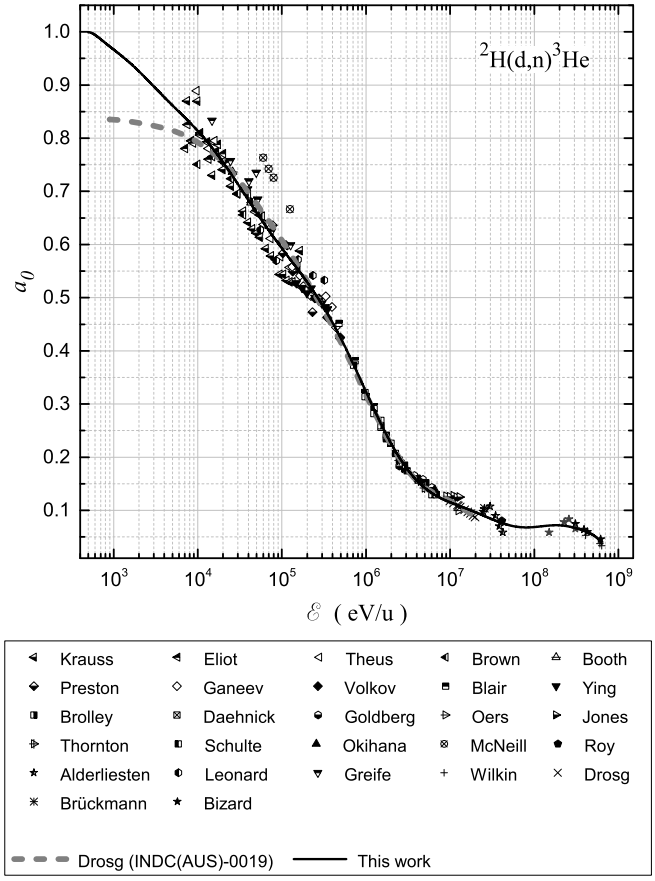

Graph 4. Normalized Legendre coefficient a_0 for ^{2}H(d,n)^{3}He reaction.

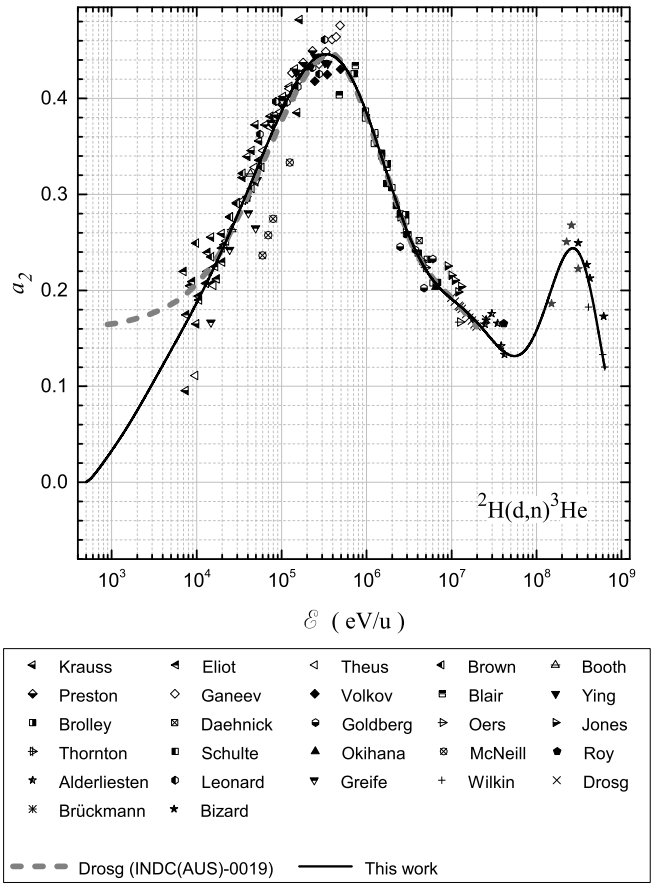

Graph 5. Normalized Legendre coefficient a_2 for ^{2}H(d,n)^{3}He reaction.

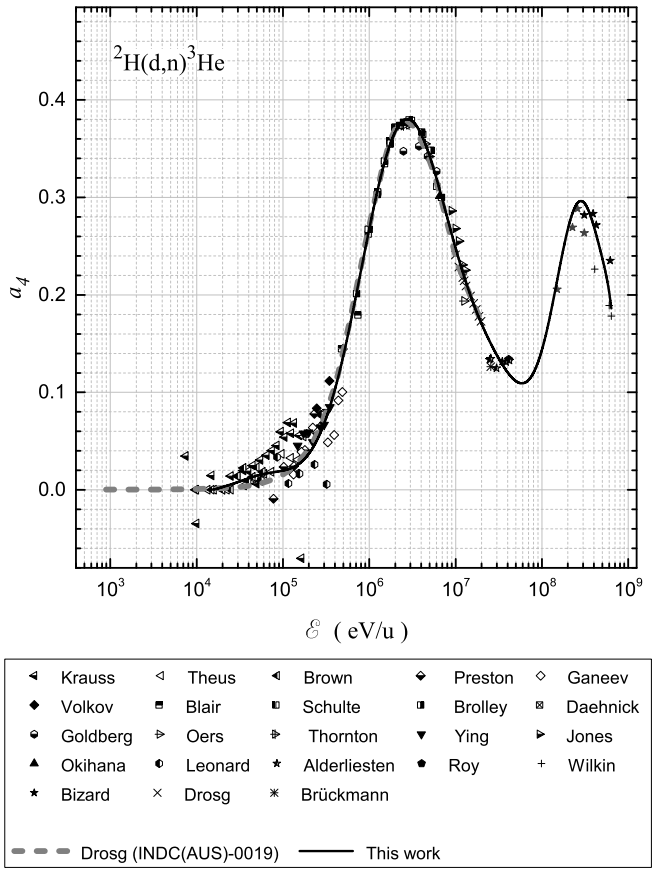

Graph 6. Normalized Legendre coefficient a_4 for ^{2}H(d,n)^{3}He reaction.

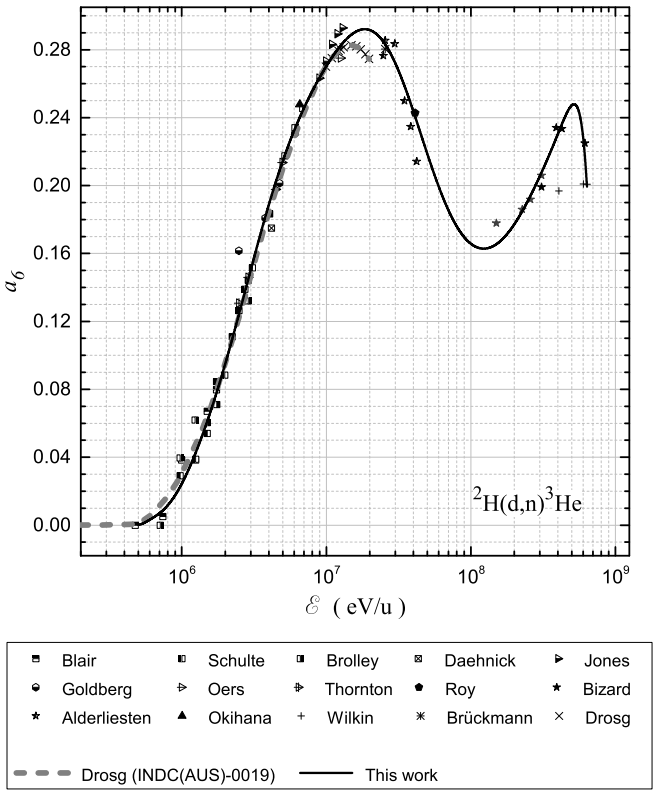

Graph 7. Normalized Legendre coefficient a_6 for ^{2}H(d,n)^{3}He reaction.

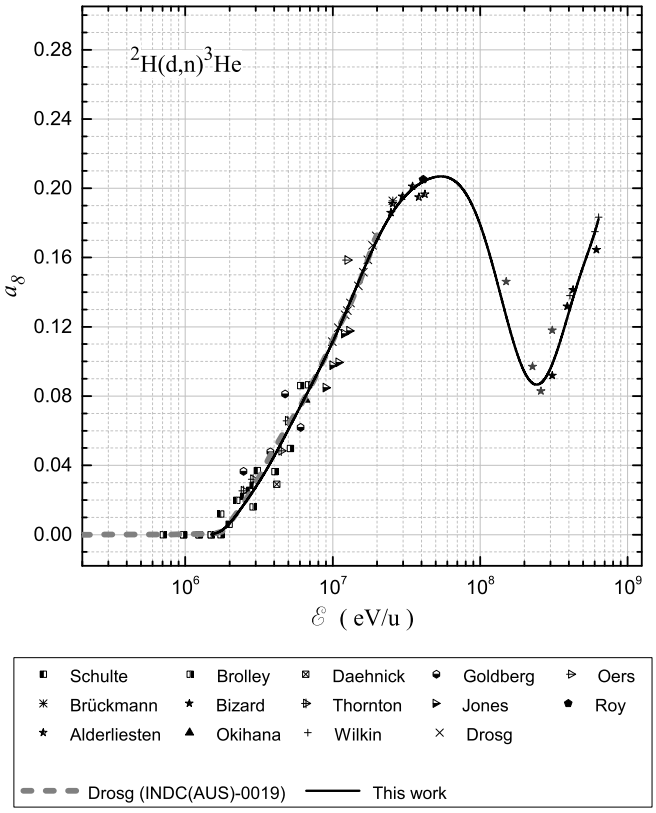

Graph 8. Normalized Legendre coefficient a_8 for ^{2}H(d,n)^{3}He reaction.

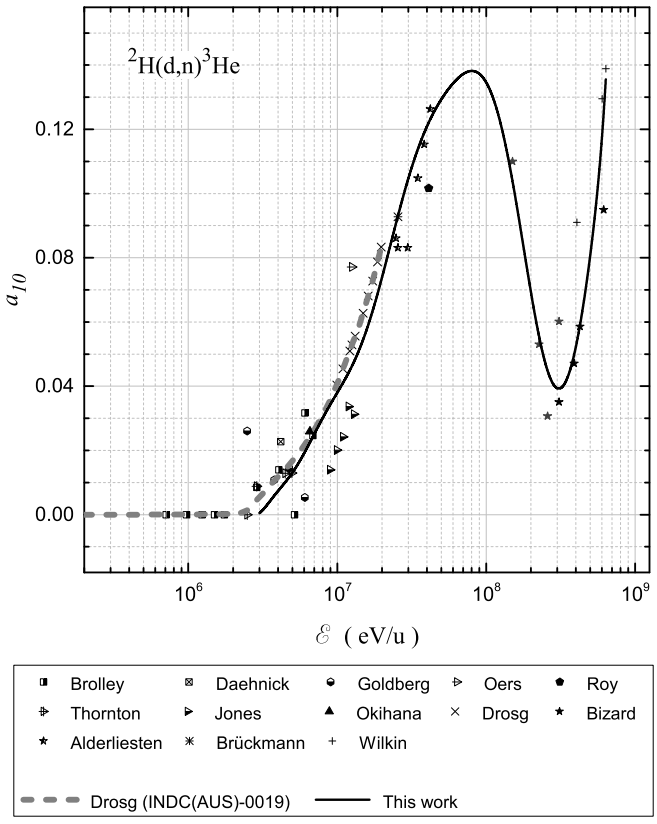

Graph 9. Normalized Legendre coefficient a_{10} for ^{2}H(d,n)^{3}He reaction.

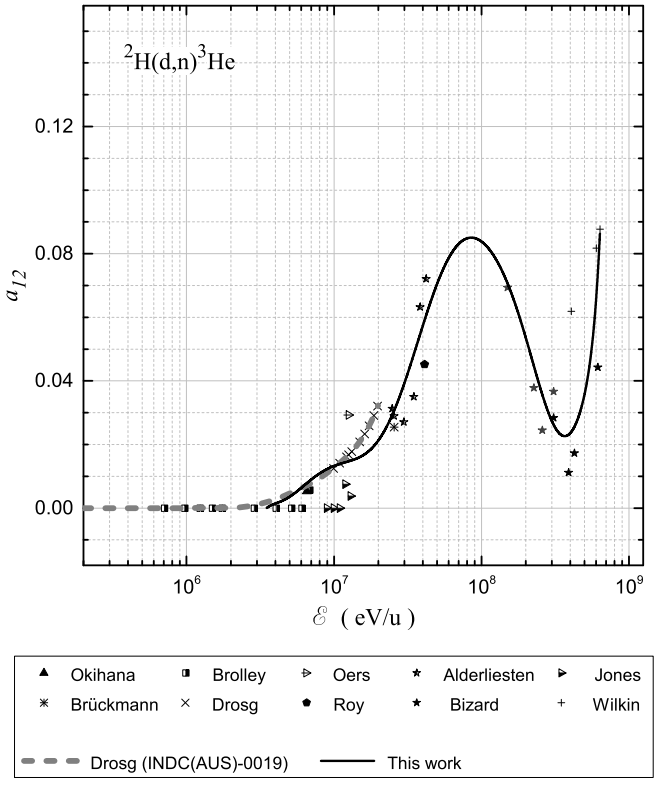

Graph 10. Normalized Legendre coefficient a_{12} for ^{2}H(d,n)^{3}He reaction.

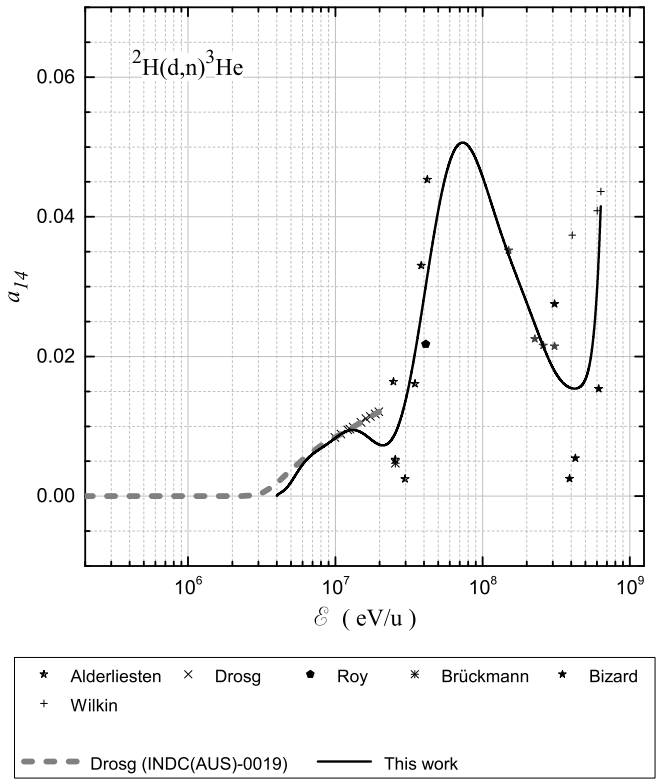

Graph 11. Normalized Legendre coefficient a_{14} for ^{2}H(d,n)^{3}He and ^{2}H(d,p)^{3}H reactions.

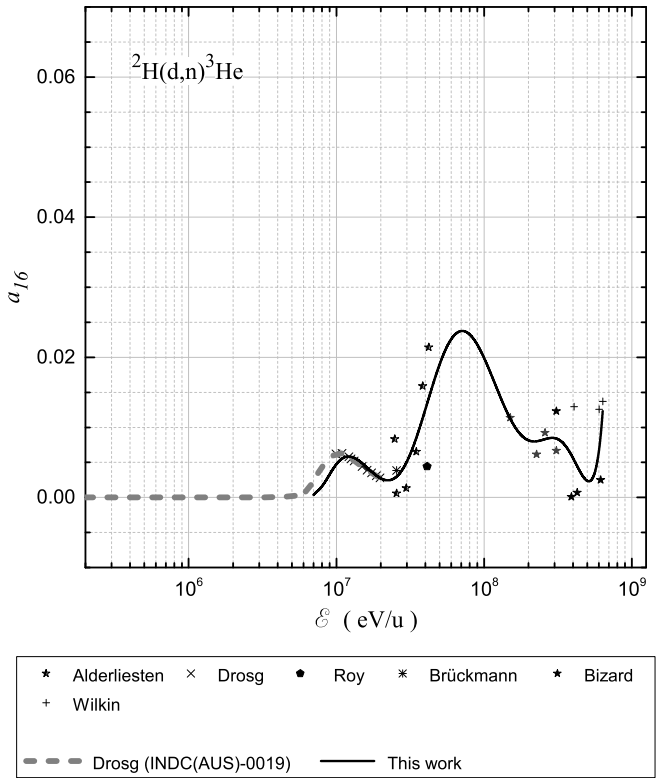

Graph 12. Normalized Legendre coefficient a_{16} for ^{2}H(d,n)^{3}He and ^{2}H(d,p)^{3}H reactions.

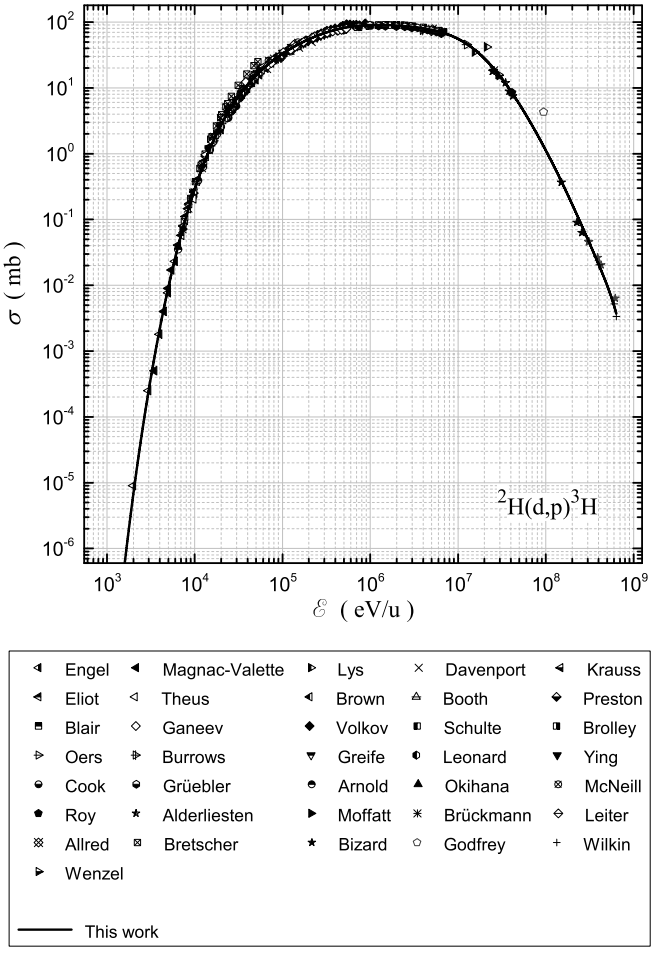

Graph 13. Total cross section of ^{2}H(d,p)^{3}H reaction.

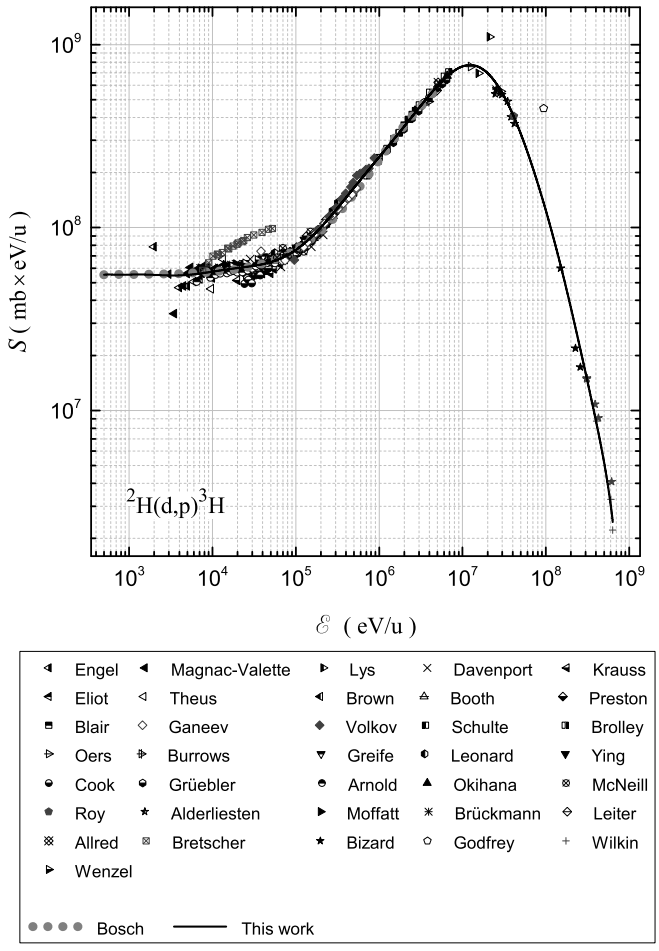

Graph 14. Astrophysical S-factor for ^{2}H(d,p)^{3}H reaction.

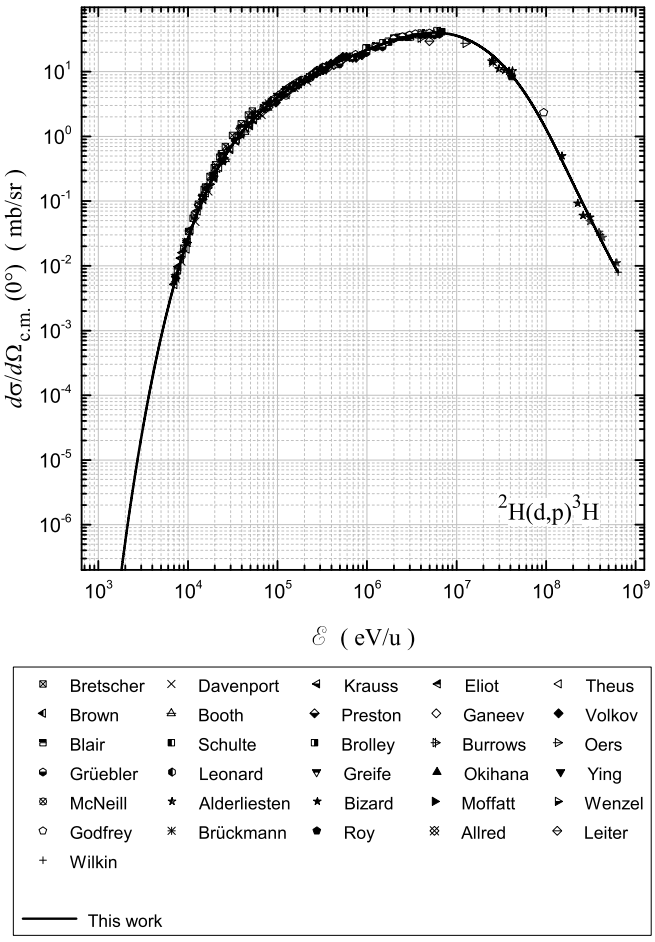

Graph 15. Differential cross section at 0° in the c.m. frame $\frac{d\sigma(\mathscr{E},0°)}{d\Omega_{\text{c.m.}}}$ for ^{2}H(d,p)^{3}H reaction.

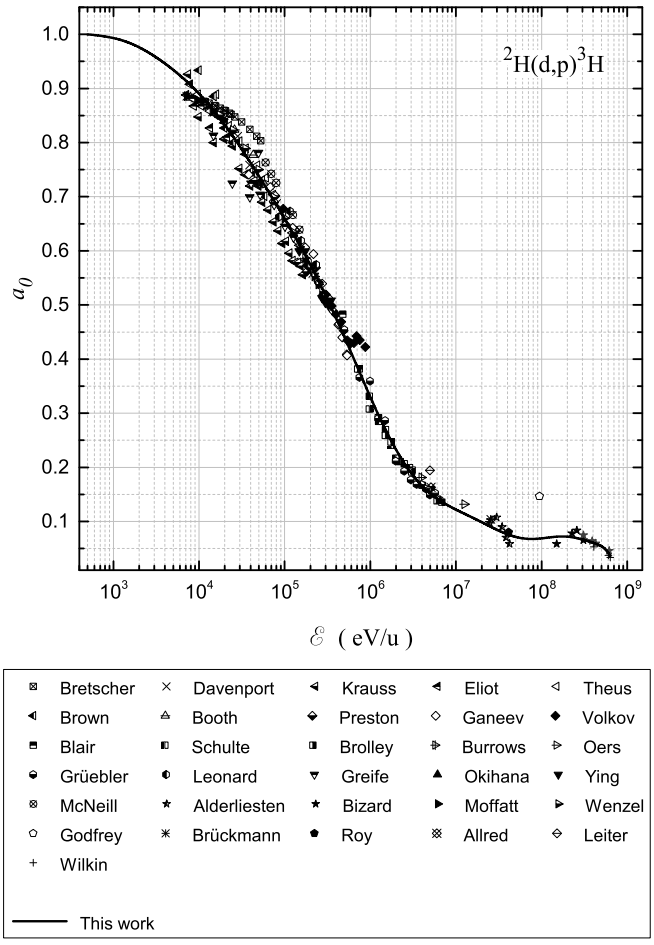

Graph 16. Normalized Legendre coefficient a_0 for ^{2}H(d,p)^{3}H reaction.

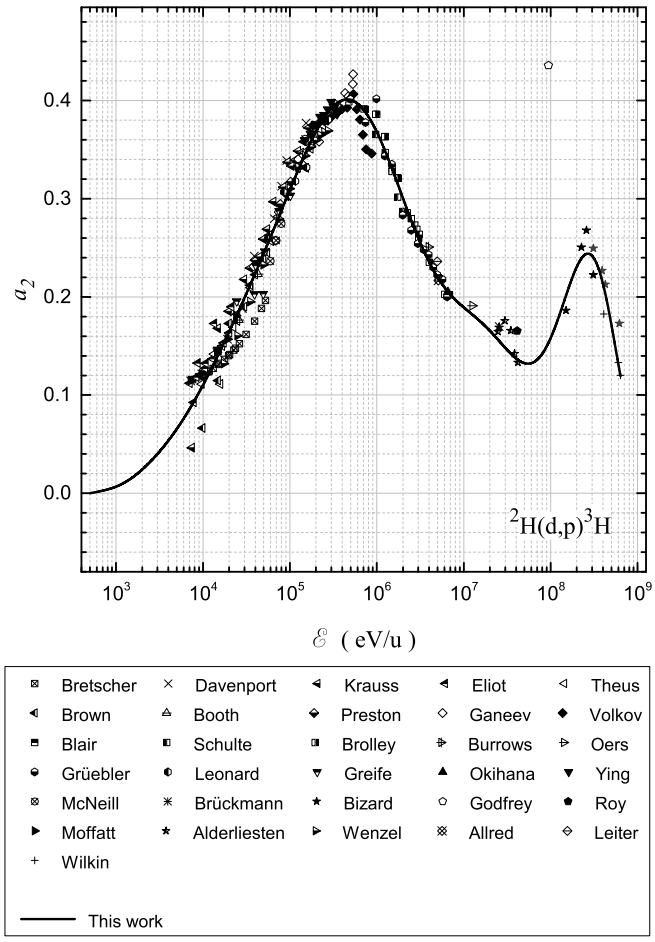

Graph 17. Normalized Legendre coefficient a_2 for ^{2}H(d,p)^{3}H reaction.

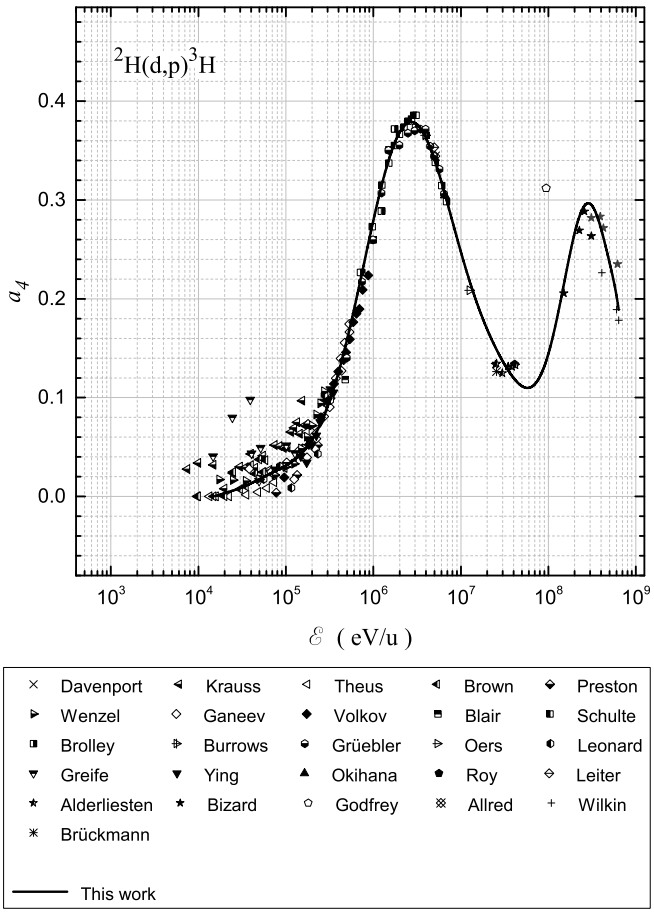

Graph 18. Normalized Legendre coefficient a_4 for ^{2}H(d,p)^{3}H reaction.

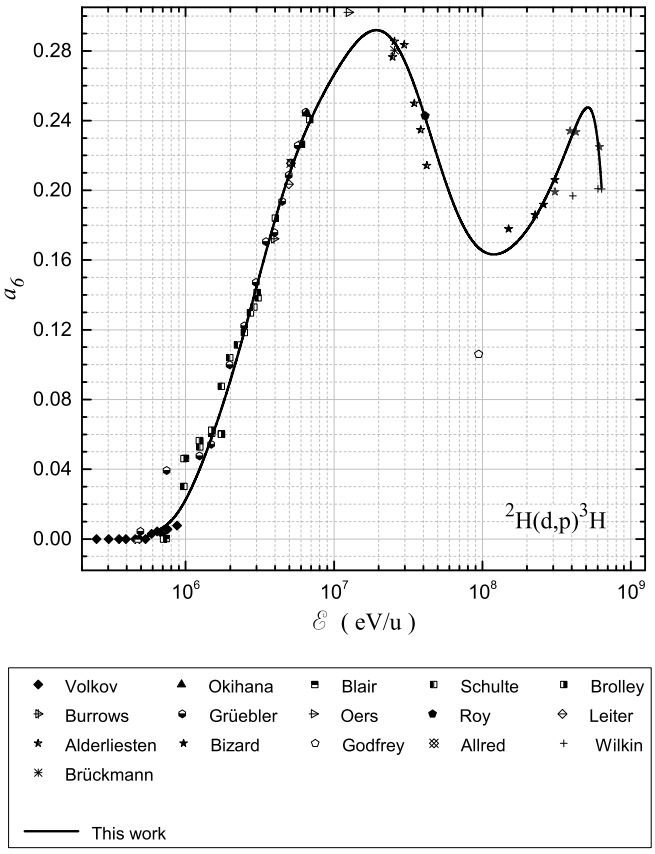

Graph 19. Normalized Legendre coefficient a_6 for ^{2}H(d,p)^{3}H reaction.

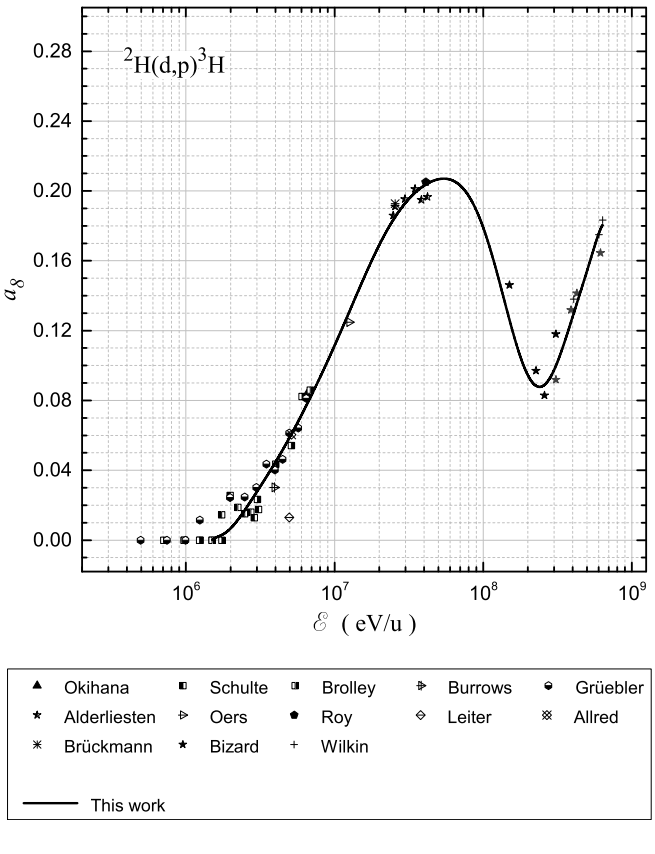

Graph 20. Normalized Legendre coefficient a_8 for ^{2}H(d,p)^{3}H reaction.

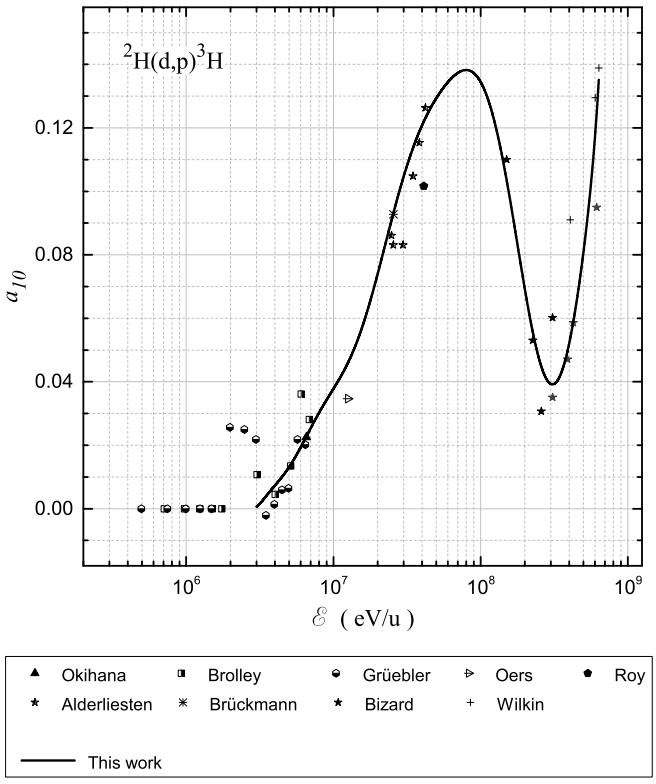

Graph 21. Normalized Legendre coefficient a_{10} for ^{2}H(d,p)^{3}H reaction.

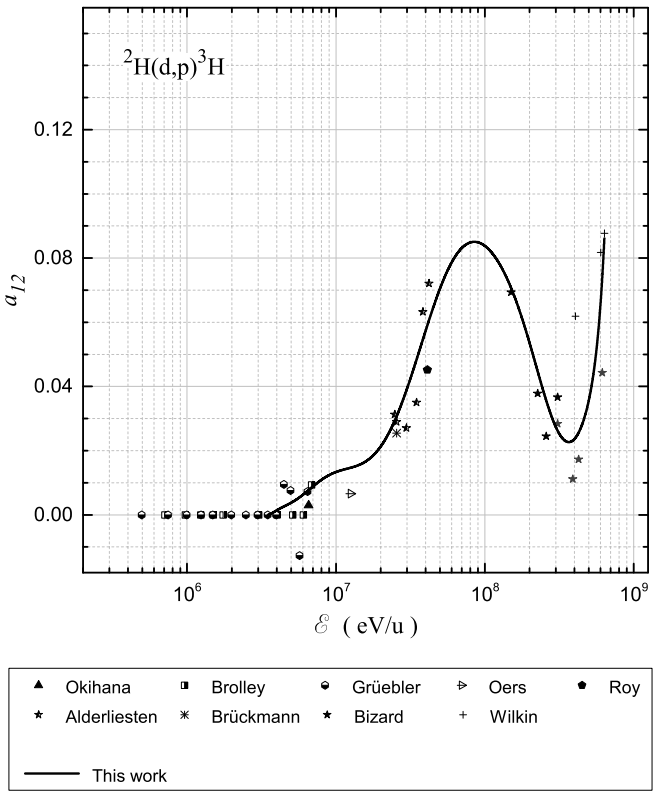

Graph 22. Normalized Legendre coefficient a_{12} for ^{2}H(d,p)^{3}H reaction.

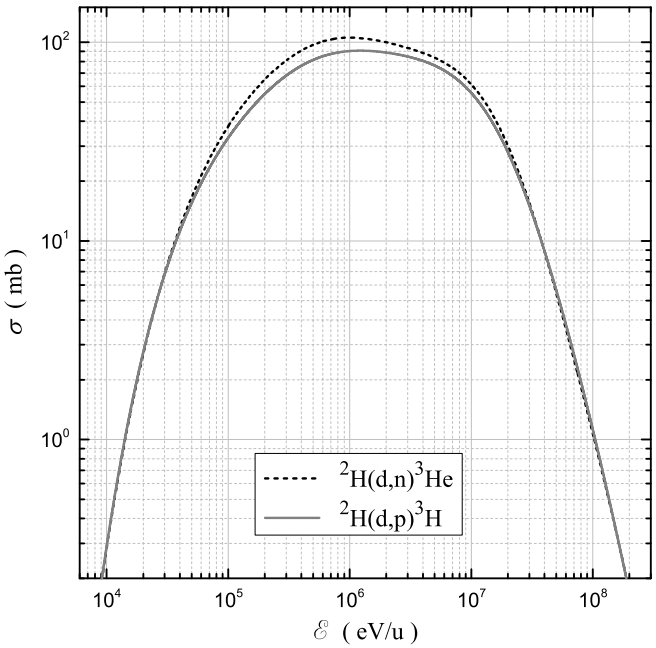

Graph 23. Total cross sections of ^{2}H(d,n)^{3}He (black dashed curve) and ^{2}H(d,p)^{3}H (gray solid curve) reactions calculated using Chebyshev coefficients from Tables 1 and 3 correspondingly.

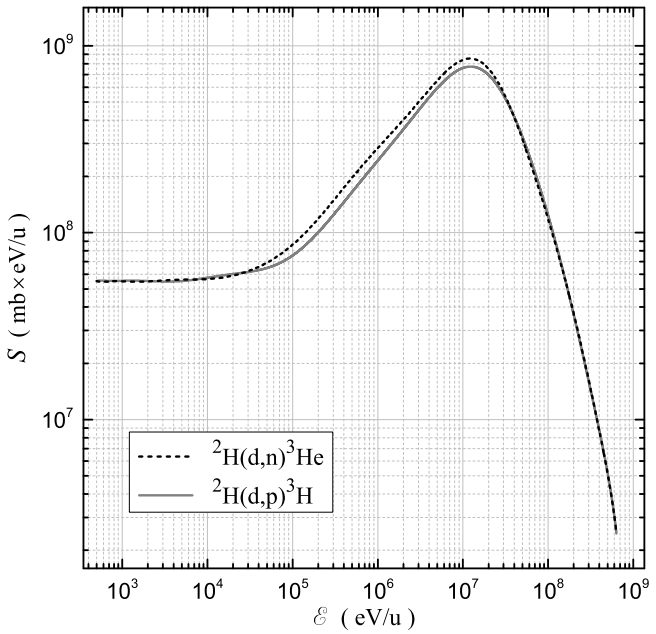

Graph 24. Astrophysical *S*-factors for ^{2}H(d,n)^{3}He (black dashed curve) and ^{2}H(d,p)^{3}H (gray solid curve) reactions calculated using Chebyshev coefficients from Tables 1 and 3 correspondingly.

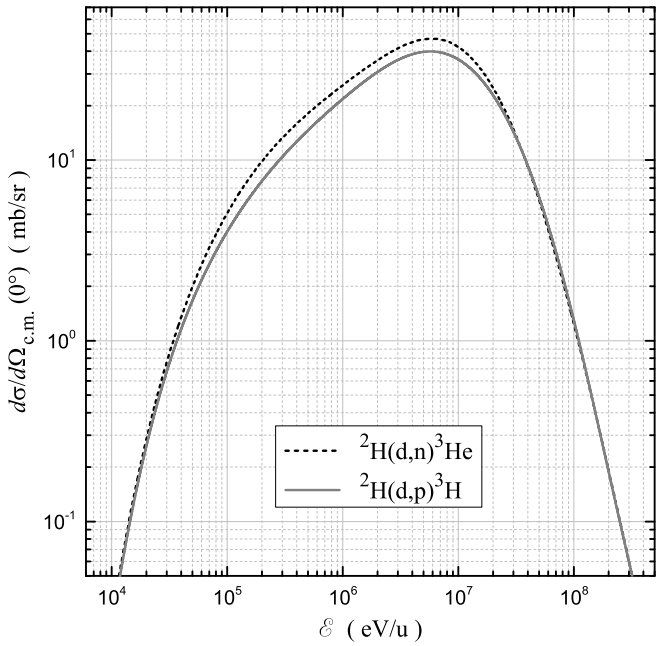

Graph 25. Differential cross sections at 0° in the c.m. frame $\frac{d\sigma(\mathscr{E},0°)}{d\Omega_{c.m.}}$ for ^{2}H(d,n)^{3}He (black dashed curve) and ^{2}H(d,p)^{3}H (gray solid curve) reactions calculated using Chebyshev coefficients from Tables 1 and 3 correspondingly.

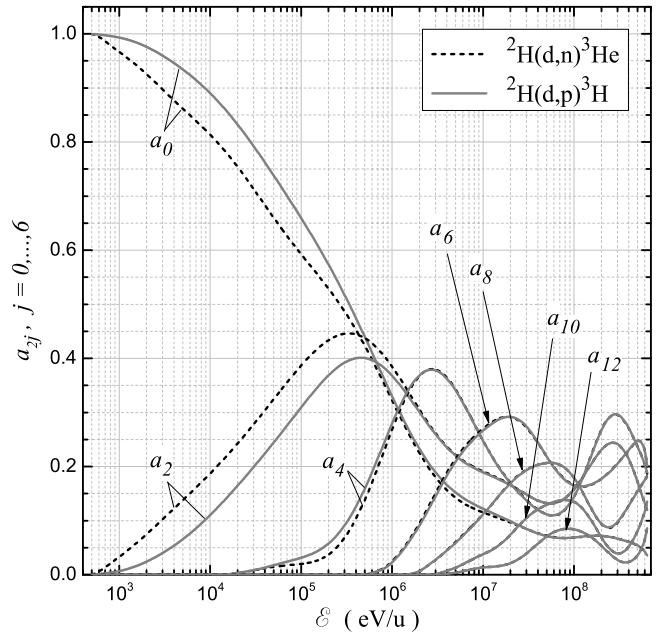

Graph 26. Normalized Legendre coefficients a_{2j} for $j = 0, \ldots, 6$ for ^{2}H(d,n)^{3}He (black dashed curves) and ^{2}H(d,p)^{3}H (gray solid curves) reactions calculated using Chebyshev coefficients from Tables 2 and 4 correspondingly.

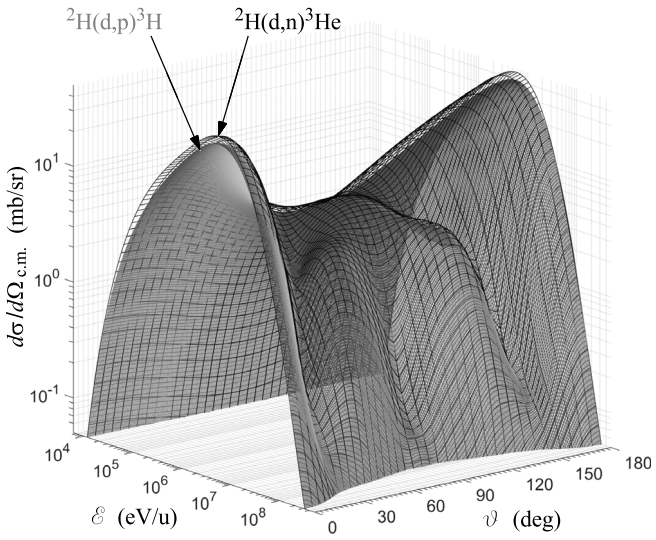

Graph 27. Differential cross sections in the c.m. frame for ^{2}H(d,n)^{3}He (black mesh) and ^{2}H(d,p)^{3}H (gray surface) reactions calculated using Chebyshev coefficients from Tables 1–4.